HiRes/MIA Measurements of Extensive Air Shower Development between 10^{17} and 10^{18}eV: Detector Description and Performance

T.Abu-Zayyad[2], K.Belov[2], D.J.Bird[5], J.Boyer[4], Z.Cao[2], M.Catanese[3], G.F.Chen[2], R.W.Clay[5], C.E.Covault[1], J.W.Cronin[1], H.Y.Dai[2], B.R.Dawson[5], J.W.Elbert[2], B.E.Fick[1], L.F.Fortson[1a], J.W.Fowler[1], K.G.Gibbs[1], M.A.K.Glasmacher[7], K.D.Green[1], Y.Ho[4], A.Huang[2], C.C.Jui[2], M.J.Kidd[6], D.B.Kieda[2], B.C.Knapp[4], S.Ko[2], C.G.Larsen[2], W.Lee[4], E.C.Loh[2], E.J.Mannel[4], J.Matthews[7b], J.N.Matthews[2], B.J.Newport[1], D.Nitz[7c], T.A.O'Halloran[6], R.A.Ong[1], K.M.Simpson[5], J.D.Smith[2], D.Sinclair[6], P.Sokolsky[2], P.Sommers[2], C.Song[4], J.K.K.Tang[2], S.B.Thomas[2], J.C.van der Velde[7], L.R.Wiencke[2], C.R.Wilkinson[5], S.Yoshida[2] and X.Z.Zhang[4]

[1] *Enrico Fermi Institute, University of Chicago, Chicago IL 60637 USA*
[2] *High Energy Astrophysics Institute, University of Utah, Salt Lake City UT 84112 USA*
[3] *Iowa State University, Ames IA 50011 USA*
[4] *Nevis Laboratory, Columbia University, Irvington NY 10533 USA*
[5] *University of Adelaide, Adelaide S.A. 5005, Australia*
[6] *University of Illinois at Champaign-Urbana, Urbana IL 61801 USA*
[7] *University of Michigan, Ann Arbor MI 48109 USA*
[a] *joint appt. with The Adler Planetarium and Astronomy Museum, Astronomy Dept., Chicago, IL 60605*
[b] *current address: Dept. of Physics and Astronomy, Louisiana State University, Baton Rouge, LA 70803 and Dept. of Physics, Southern University, Baton Rouge, LA 70801 USA*
[c] *current address: Dept. of Physics, Michigan Technical University, Houghton, MI 49931 USA*

Abstract

The HiRes prototype detector was operated for almost three years in coincidence with the CASA and MIA EAS arrays. We are able to extract mass composition information from the HiRes data (the shower depth of maximum) and from the MIA data (the muon content). In this paper we describe the detectors and their ability to measure mass composition parameters. Physics conclusions and their sensitivity to systematic effects are described in an accompanying paper (Abu-Zayyad et al. 1999).

1   Introduction:

The HiRes prototype detector operated from September 1993 to May 1996 and viewed the sky above the CASA/MIA arrays. An attractive physics study for the prototype was the cosmic ray mass composition, using information from the HiRes detector and the MIA muon array. Because of the limited collecting area the energy range studied was rather narrow, from 10^{17}eV to 10^{18}eV, but the data were unique with coincident measurements of longitudinal development and muon content, both sensitive to mass composition.

The HiRes prototype detector (Bird et al. 1993) consisted of 14 mirrors viewing an elevation range of $3° - 70°$ in the direction of CASA/MIA arrays centered 3.4 km away. HiRes observes the nitrogen fluorescence light induced by an EAS, and can therefore reconstruct the longitudinal development of the shower. The energy of the primary can then be extracted (Song et al. 1999) and the depth of maximum, $X_{\max}$, determined.

The MIA array has been described in detail by Borione et al. (1994). It is an array of 1024 buried muon detectors arranged in 16 patches of 64 detectors each. Over $2400\,\mathrm{m}^2$ of muon detector area is distributed over the total array area of $0.25\,\mathrm{km}^2$. The muon threshold energy is approximately $0.75\sec\theta\,\mathrm{GeV}$ where θ is the zenith angle of the EAS.

The HiRes events were matched with CASA or MIA triggers if either of the array trigger times were within $3\,\mathrm{ms}$ of a HiRes trigger, or if the arrays received a light flasher signal from HiRes within $50\,\mu\mathrm{s}$ of the array trigger (Bird et al. 1995). In addition we require that there be at least 80 muon hits for events with both CASA
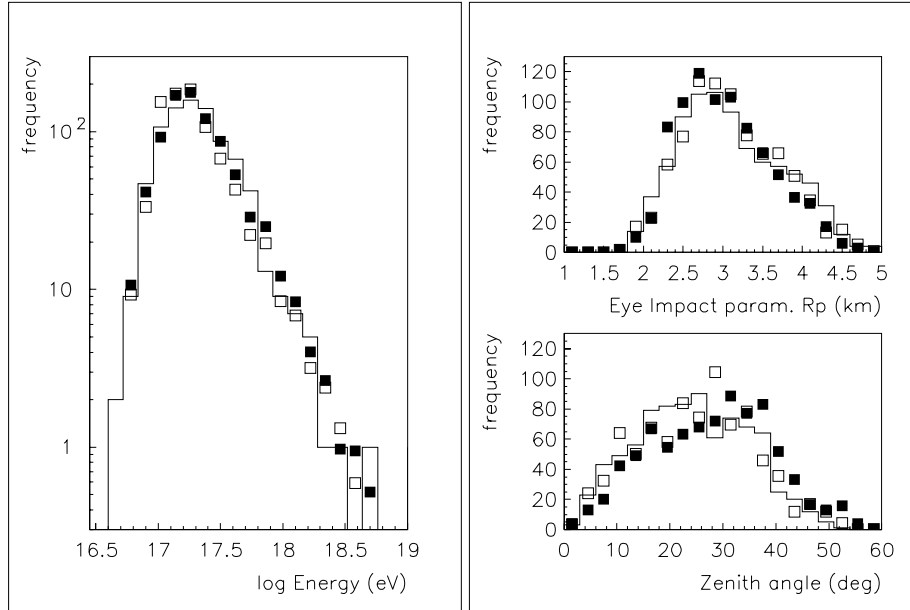
Figure 1: Distributions of 894 real events (histograms) seen by the HiRes prototype and the MIA array. Quality cuts have been applied to the data and the simulated proton showers (solid squares) and iron showers (open squares). Simulated histograms have the same area as the data distributions. See text for discussion.

and MIA triggers and 40 muon hits with a MIA trigger alone. Almost 2500 coincident events passed through the reconstruction procedures, representing an analysed event rate close to 1 per hour.

2 Simulation Procedure:

The CORSIKA package has been used to simulate proton and iron initiated EAS at a number of fixed energies between $10^{16.5}$ and $10^{18.7}$ eV over a range of zenith angles (Song et al. 1999). From the CORSIKA output, parametrizations of shower development were produced to provide profile parameters for any primary energy in this range, with a realistic treatment of fluctuations. In addition, the muon lateral distribution and the muon arrival time distribution (ie shower front thickness) were parametrized as a function of energy and zenith angle for both primary species, again with a careful treatment of fluctuations. Parametrizations were developed for both the QGSJET and the SIBYLL hadronic interaction models.

A detector Monte Carlo program was developed to use these parametrizations to simulate the response of the HiRes prototype and the MIA array. The data files generated are identical to those produced by the real experiment, and are analysed using the standard analysis programs.

The HiRes prototype simulation begins with light production at the shower. Fluorescence and Cerenkov light is simulated in 16 wavelength bands (300 - 400 nm), with the former using the most up to date efficiencies for the scintillation process (Kakimoto et al. 1996). Rather than treating the shower as a line source of light, we use an age-dependent NKG lateral distribution to provide width to the emitting region. The observed Cerenkov light may come directly from the shower, or it may be seen after suffering single Rayleigh or aerosol scattering. Light transmission from the shower to the detector is simulated, taking account of absorption (small) and scattering. The aerosol scattering parameters (mean free path, scale height, phase function) may be varied.

The detector optics are treated using parametrizations of full raytracing, including the effect of non-uniform photocathode efficiency (an average response function was assumed for all pmts) and the loss of light in gaps between pmts. For every pmt viewing light, the electronics pulse shaping and triggering are simulated, including the effects of night sky background light, and the timing systematic known as time slewing (ie late

triggering for small pulses). Data from the real experiment on the triggering threshold in each mirror is used. The output information is the triggering time of each triggered pmt, together with the photoelectron integral within the 1.2 μs integration period.

The MIA array simulation takes account of particle number fluctuations, dead counters, counter efficiencies (taken to be 93%), trigger formation and the time windows for accepting counter hits, noise muons, and pulse risetimes. The output from this part of the simulation specifies the hit counters and the trigger time of the last muon to trigger each of those counters.

3 Analysis Procedure:

The analysis chain is identical for simulated data and real data. First, the geometrical analysis is performed, where we determine the EAS axis position and the muon parameters. A hybrid method is used, where information from HiRes and MIA is combined to provide a well constrained track position and direction. Simply put, the procedure starts with an estimate of the shower-detector plane (SDP), defined by the position of the eye and the directions of the triggering HiRes pmts. The position and angle of the EAS axis within this plane is then determined using the HiRes pmt trigger times in conjunction with the direction determined by a fit to the muon timing data. The muon size is determined assuming a lateral distribution of the AGASA form (Hayashida et al. 1995). The integrated muon size N_μ and the density 600 m from the core $\rho(600)$ are estimated.

The next procedure determines the number of photoelectrons received from the shower by HiRes as a function of angle along the axis, in $1°$ bins. It combines signals from pmts and thereby take account of the lateral width of the source (the shower), the aberrations in mirror optics, variations of the pmt efficiency across their surfaces, and gaps in the focal plane. In practice, the procedure takes the SDP determined previously, and makes small shifts to this plane in each mirror to get the best agreement between the measured signal amplitudes and those predicted for a trial track brightness.

The final procedure takes the "binned" photoelectron signal and searches for the best fit shower longitudinal profile. Here, a trial profile is simulated with the nominal geometry, and the light received at the detector is calculated using many of the techniques described above for the HiRes simulation. We assume a Gaisser-Hillas form for the shower profile, with fixed values of $X_o = -20\mathrm{g/cm}^2$ and $\lambda = 70\mathrm{g/cm}^2$. This analysis results in estimates of $X_{\max}$ and the shower energy. The energy assignment includes a correction for the fraction of shower energy that does not fully participate in fluorescence production (Song et al. 1999).

Figure 2: Resolution plots for simulated QGSJET iron showers. Simulations were generated with a E^{-2} differential spectrum and subsequently weighted to represent a E^{-3} spectrum. Standard cuts (see text) have been applied. The energy histogram represents $(E_{out} - E_{in})/E_{in}$.

4 Results:

All simulations described here were generated with a spectrum of trial energies from 3×10^{16} to 5×10^{18} eV with an differential spectral index of -2.0, a unit flatter than the real spectrum. After analysis, weighting was applied to the simulated data to retrieve the proper -3.0 spectral index. Thus all resolution figures given below will apply to a realistic sample of events over a full energy range.
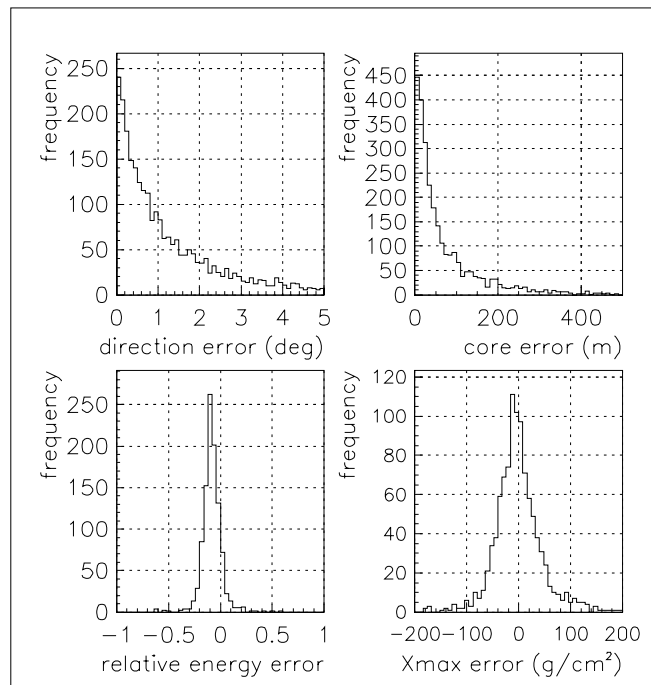
The hybrid triggering aperture (eye + MIA) is approximately independent of the particle species (iron or proton) and the interaction model. At the lowest energies, the slightly lower HiRes triggering efficiency for iron showers compared with proton showers is balanced by an opposite bias in the muon array. The hybrid trigger aperture rises from $1\,\mathrm{km}^2\mathrm{sr}$ at $10^{17}\mathrm{eV}$ to $5\,\mathrm{km}^2\mathrm{sr}$ at $10^{17.5}\mathrm{eV}$ and $6\,\mathrm{km}^2\mathrm{sr}$ above $10^{18}\mathrm{eV}$.

The simulated data were generated assuming an atmosphere with an aerosol content specified by a $10\,\mathrm{km}$ horizontal attenuation length at $350\,\mathrm{nm}$; a $1.2\,\mathrm{km}$ aerosol scale height; no aerosol mixing layer; and a simple scattering phase function. Our sensitivity to these choices is explored in .Abu-Zayyad et al. (1999).

The data quality cuts are: 1) angular track length $> 20°$; 2) MIA core distance $< 2\,\mathrm{km}$; 3) uncertainty in $X_{\max}$ due to geometrical errors and profile fitting are both $< 50\,\mathrm{g/cm}^2$; 4) visible track is longer than $250\,\mathrm{g/cm}^2$; 5) shower maximum is viewed; 6) the χ^2 for the profile fit < 10 and 7) the minimum viewing angle (the angle between the pmt line of sight and the shower axis) in an event must be larger than $10°$.

Figure 1 shows the data distributions for energy, impact parameter and zenith angle. The cuts result in 838 real events. We compare these distributions with those predicted from simulations for proton and iron primaries. We see that the shape and threshold of the energy distribution is well predicted. The zenith angle distribution shows a difference between proton and iron primaries. With the requirement that the detector see $X_{\max}$, proton showers are slightly biased to larger zenith angles compared with iron showers.

Figure 2 shows the reconstruction resolution for iron showers. Distributions for proton showers are similar, except that the bias in the energy resolution is positive rather than negative. The bias is due to the correction applied to the reconstructed energy to account for "missing" energy carried by high energy muons, neutrinos and low energy gamma-rays that isn't accounted for in the calorimetric method (Song et al. 1999). We apply a correction to all data which is an average of the proton correction and the iron correction; thus simulated iron showers are under-compensated and proton showers are over-compensated.

Table 1 summarises the resolution figures for proton and iron showers generated with the QGSJET interaction model and a E^{-3} differential spectrum. The width of the resolution function and its offset are given. Depth of maximum is measured with a resolution of approximately

QGSJET	proton		iron	
	σ	mean	σ	mean
E (%)	16	13	10	-8
$X_{\max}$ (g/cm^2)	44	7	44	-2
X_{core} (m)	42	-2	40	-1
Y_{core} (m)	57	-2	55	2
N_μ (%)	30	-7	30	-4
N_μ (%)*	19	-7	19	-6
space angle	0.88°		0.83°	

Table 1: Resolution figures for a E^{-3} differential spectrum seen by HiRes and MIA. Standard quality cuts have been applied. For * an additional cut requiring 80 muon hits has been applied. Space angle errors are median values.

$40\,\mathrm{g/cm}^2$. The geometry of these close-by showers means that we do not view a large grammage range, resulting in a poorer resolution than would be expected for more distant showers. The N_μ resolution is given for the standard cuts, plus an additional cut of demanding greater than 80 muon hits in the event. In all cases it appears that muon sizes are being underestimated by 5-10%. This is related to the choice of a fixed lateral distribution function in the analysis.

The conclusions from this study are described in an accompanying paper (Abu-Zayyad et al. 1999).

References

Abu-Zayyad, T. et al. 1999, OG 4.5.07 (these proceedings)
Bird, D.J. et al. 1993, Proc. 23rd ICRC (Calgary) 2, 462
Bird, D.J. et al. 1995, Proc. 24th ICRC (Rome) 2, 760
Borione, A. et al. 1994, Nucl. Inst. and Meth. A346, 329
Hayashida, N. et al. 1995, J.Phys.G. 21, 1101
Kakimoto, F. et al. 1996, Nucl. Inst. and Meth. A372, 527
Song, C. et al. 1999, OG 4.5.09 (these proceedings)